Technical Paper

ISSN 1997-1400 Int. J. Pavement Res. Technol. 7(3):178-184

Numerical Analysis of Surface Crack Propagation in Flexible Pavements Using XFEM and Cohesive Zone Model

Hao Wang[1+] and Jian Wang[1]

Abstract: Surface initiated **(**top-down) cracking in the longitudinal direction of pavements has become a predominant mode of failure in thick asphalt pavements. Most previous researchers studied crack propagation using the traditional Linear Elastic Fracture Mechanics (LEFM) method by calculating the stress intensity factor around the crack tip. In this paper, Extended Finite Element Method (XFEM) was used to study the key factors causing surface initiated crack propagation under surface tension and/or shear. A two-dimensional (2-D) finite element (FE) model for a two-lane flexible pavement was built to predict pavement responses and crack propagation potential under various scenarios. It was found that surface tension is the major driving force for crack propagation when the crack is at some distance away from tire loading. The results show that the distance from the location of crack to tire loading, the depth and direction of the crack, and the modulus ratio between the hot-mix asphalt (HMA) layer and the base layer have significant influences on crack propagation under surface tension. On the other hand, this study shows that shear stress can induce surface initiated crack propagation near the loading area as the shear resistance of material becomes low at the high temperature.

DOI:10.6135/ijprt.org.tw/2014.7(3).178
***Key words**: Cohesive zone model; extended finite element method; flexible pavement; surface initiated cracking.*

Introduction

Traditionally, the critical cracking failure in flexible pavements is the crack initiated at the bottom of the hot-mix asphalt (HMA) layer. However, field observations of cores and trench sections from in-service pavements have shown that premature failures may develop from the surface and propagate their way down, such as top-down cracking [1-2]. Recently, it was found that the crack could also initiate from the near-surface of thick asphalt pavements [3-5].

Surface initiated cracking in pavements is a complex process because it is affected by many factors including tire-pavement contact stresses, HMA material properties, layer thickness, and etc. Over the last decades many numerical models have been proposed to study the fracture mechanism in flexible pavements such as linear and nonlinear fracture model, cohesive zone model, and smeared cracking model. The cohesive zone model (CZM) has proved to be a very effective tool to simulate crack propagation of asphalt material [6-7]. Compared to traditional linear elastic fracture mechanics, CZM has advantages in modeling brittle and ductile failures with plastic zone at the crack tip that are common in asphalt materials. However, the major disadvantage of cohesive zone model is that the crack propagation path needs to be known a priori in which the cohesive element is inserted. Therefore, the conventional finite element model (FEM) with CZM cannot predict the randomly developed crack and its propagation path.

Recently, extended finite element method (XFEM) was introduced to overcome the limitation of crack propagation along the predefined path [8]. The advantage of XFEM is to simulate arbitrary crack initiation and propagation without changing the mesh and geometry of the model. Since the XFEM is relatively new, few researches have been conducted to model pavement cracking using XFEM. Ozer *et al*. (2011) performed 3-D analysis of near-surface cracking using the generalized finite element method (GFEM) and calculated stress intensity factors of stationary cracks at various locations [9]. Similarly, Garzon, *et al*. (2010) analyzed reflective cracks in airfield pavements using the stress intensity factors under various gear loading conditions that were calculated using GFEM [10]. The GFEM is based on partition of unity and has the same features as XFEM [11]. However, no crack propagation is considered in the above studies.

The focus of this study is to analyze the propagation behavior of surface initiated cracking in the asphalt pavement using XFEM. A finite element model was developed using the commercial FE software ABAQUS. By comparing the results under various scenarios, the critical factors that contribute most to crack propagation were identified. The factors considered in this study mainly include the location and geometry (length, depth and angle) of the initial crack, the stiffness of pavement layers (modulus and thickness), and the influences of crack opening modes (tension and shear). This study concentrated on crack propagation not initiation by assuming a single crack already developed at the surface or near-surface of an asphalt pavement.

Extended Finite Element Method with Cohesive Zone Model

Extended finite element method (XFEM) is a mesh independent finite element fracture modeling approach in which the FE mesh is generated independent of the crack, and the crack path and location are not specified. The extended finite element method is an extension of the conventional finite element method based on the concept of partition of unity, which allows local enrichment

[1] Department of Civil and Environmental Engineering, Rutgers, The State University of New Jersey, Piscataway, NJ, 08854, USA.
[+] Corresponding Author: E-mail hwang.cee@rutgers.edu
Note: Submitted June 21, 2013; Revised November 30, 2013; Accepted December 31, 2013.

functions to be easily incorporated into a finite element approximation [12].

In the XFEM, the presence of discontinuities is ensured by the special enriched functions in conjunction with additional degrees of freedom. For the purpose of fracture analysis, the enrichment functions typically consist of the near-tip asymptotic functions that capture the singularity around the crack tip and a discontinuous function that represents the jump in displacement across the crack surfaces. The approximation for a displacement vector function with the enrichment is shown in Eq. (1).

$$u = \sum_{I=1}^{N} N_I(x)\left[u_I + H(x)a_I + \sum_{\alpha=1}^{4} F_a(x)b_I^{\alpha} \right] \quad (1)$$

where $N_I(x)$ are the usual nodal shape functions; u_I, is the usual nodal displacement vector associated with the continuous part of the finite element solution; a_I, and the associated discontinuous jump function $H(x)$ across the crack surfaces; and b_I^{α}, and the associated elastic asymptotic crack-tip functions, $F_a(x)$. The first term on the right-hand side is applicable to all the nodes in the model; the second term is valid for nodes whose shape function support is cut by the crack interior; and the third term is used only for nodes whose shape function support is cut by the crack tip.

In ABAQUS, when the crack propagation is simulated using XFEM, the near-tip asymptotic singularity (the third term on the right-hand side in Eq. (1)) is not needed, and only the displacement jump across a cracked element (the second term on the right-hand side in Eq. (1)) is considered. Therefore, the crack has to propagate across an entire element at a time to avoid the need to model the stress singularity. The level set method [13] is used with the XFEM to model arbitrary crack growth without re-mesh. Phantom nodes, which are superposed on the original real nodes, are used to represent the discontinuity of the cracked elements [14]. The phantom node is completely constrained to its corresponding real node when the element is intact; while the phantom node splits from the real node when the element is cut through by a crack.

Cohesive zone elements with linear softening were used to simulate crack propagation along an arbitrary, solution-dependent path at the crack tip. Cohesive zone elements open when there is damage growth to simulate crack initiation or crack propagation. Crack initiation refers to the beginning of degradation of the cohesive response at an enriched element. The process of degradation begins when the stresses or the strains satisfy the specified crack initiation criteria. The maximum nominal stress criterion was used in this study, Eq. (2). The damage is assumed to initiate when the maximum nominal stress ratio reaches a value of 1.

$$\max\left\{ \frac{<t_n>}{t_n^0}, \frac{t_s}{t_s^0}, \frac{t_t}{t_t^0} \right\} = 1 \quad (2)$$

where t_n^0, t_s^0, and t_t^0 represent the peak values of the nominal stress in the normal, the first, and the second shear directions, respectively; t_n, t_s, and t_t are the stress required to cause failure in the normal, the first, and the second shear directions, respectively, respectively.

Damage evolution could be characterized by an energy approach. The dependence of the fracture energy at a mix-mode can be defined based on a power law fracture criterion, Eq. (3). The power law criterion states that failure is governed by a power law interaction of the energies required to cause failure at a mix-mode (normal and shear).

$$\left\{ \frac{G_n}{G_n^c} \right\}^{\alpha} + \left\{ \frac{G_s}{G_s^c} \right\}^{\alpha} + \left\{ \frac{G_t}{G_t^c} \right\}^{\alpha} = 1 \quad (3)$$

where G_n, G_s, and G_t refer to the work done by the traction and its conjugate relative displacement in the normal, the first, and the second shear directions, respectively; G_n^C, G_s^C, G_t^C are the critical fracture energies required to cause failure in the normal, the first, and the second shear directions, respectively; and α is the power parameter.

It is noted that Status_XFEM is a parameter used in ABAQUS that indicates the crack status of the element with a value between 0.0 and 1.0 [15]. A value of 1.0 indicates that the element is completely cracked with no traction across the crack faces. Other values between 1.0 and 0.0 indicate that the material is partly damaged yet not fully cracked.

Finite Element Model Development

The modeled pavement structure consists of a 254-mm asphalt layer and a 300-mm stabilized soil layer placed on natural subgrade, which is a full-depth asphalt pavement section. The layer interface condition is assumed to be full-bonded and no slip is allowed between pavement layers. A relatively fine mesh was used in the HMA layer and the mesh was further refined near the loading area. The pavement material was characterized as linear elastic material and typical elastic modulus and Poisson's ratio of each layer was used. The fracture parameter of asphalt mixture was obtained from a previous study [16]. Table 1 lists the elastic and fracture parameters used in the finite element model. It is noted that the tensile strength and shear strength of HMA is assumed the same but the mode-II (shear) fracture energy is greater than the mode-I (tension) fracture energy.

Fig. 1 shows the finite element mesh of the pavement model. Two travel lanes were modeled to study the loading influence on the whole pavement section. To simplify the loading condition, only one side of a single axle load with dual tires was applied on the pavement surface. Since the focus of study is to consider the effect of surface crack location and geometry on crack propagation potential, relatively simple loading conditions were used. The tire-pavement contact stress was assumed equal to a standard tire pressure of 100 psi, and the loading area was determined by assuming a circular contact area under a 9-kip load. This is consistent with the typical loading assumption used in the mechanistic analysis of pavement responses. A roller boundary condition was applied at both sides of the pavement and a fixed boundary condition was applied at the bottom of the pavement. Initial crack was inserted by a wire element. The length and location of initial crack was varied to study theirs effects on crack propagation potential.

Table 1. Material Properties of Different Layers Used in the FEM Model.

Layer	Thickness (mm)	Modulus (MPa)	Tension and Shear Strength (MPa)	Mode-I fracture Energy Per Unit Area (N/m)	Mode-II Fracture Energy Per Unit Area (N/m)
HMA	254	5500	1.3	1.5	4.8
Base	305	300	N/A	N/A	N/A
Subgrade	N/A	100	N/A	N/A	N/A

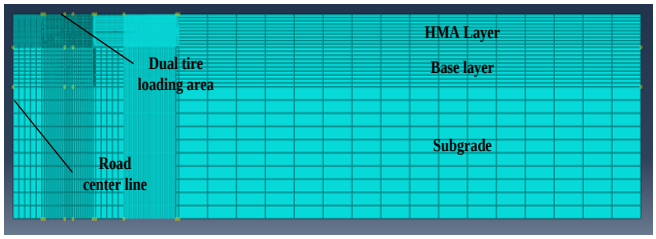

Fig. 1. Illustration of FE Mesh.

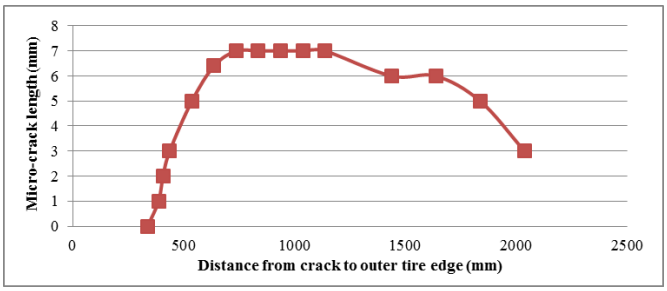

Fig. 2. Micro-crack Length Due to Tension at Different Locations.

It is known that mesh size has significant influence on the results of FEM. In general the finer the mesh is the more accurate results it will provide. Fine meshes can also reduce converging issues for nonlinear problems. However, fine meshes require more computation time and memory resource. A mesh sensitive study was conducted in this study to investigate the effect of mesh size at the crack tip on crack growth. The results show that crack growth does not vary much after the mesh is refined to a certain level. To obtain a balance between accuracy and computational time, a mesh size of 1 mm by 1 mm was used near the crack tip.

The crack length and the depth of the initial crack were assumed at the same length scale of aggregate size. The initial crack could initiate from the existing defects in the asphalt mixture such as the stone-binder interface or air void. Due to binder aging and segregation, it is possible that the initial crack will start from pavement surface or near-surface. In this study, the initial crack was assumed at different locations and the crack propagation potential was investigated. The utilization of XFEM allows the crack to be put at different locations, which eliminates meshing problems and increases the accuracy of the solution at crack fronts.

Results and Analysis

Critical Location of Crack

A standard static analysis was conducted to predict the distribution of stress and strain in the pavement without initial cracks. This offers prediction of critical locations for crack growth study. As expected, the critical tensile stress is located at the bottom of the HMA layer; this is the critical location for bottom-up cracking. However, the surface initiated cracking is affected by the stress states close to the pavement surface, which include the surface tension at some distance away from the loading area and the near-surface shear at the vicinity of tire loading. The maximum surface tensile stress was found to be 0.74 MPa; while the maximum near-surface shear stress was found to be 0.43 MPa. Although the maximum tensile/shear stress is smaller than the minimum stress required for crack propagation (tensile/shear strength), the insertion of crack would induce stress concentration and result in high tensile/shear stress at the crack tip.

To identify the critical location of surface cracking, a 15-mm initial crack was placed at various locations with respect to the tire loading area. Previous studies [17, 18] have shown that the shear-mode cracking mostly happens at the vicinity of tire edge, while the tension-model cracking usually happens at some distance away from the tire.

For the crack propagation due to surface tension, the horizontal distances from the location of crack to the outer tire edge varied from 335 mm to 2050 mm. It was found that no discrete crack was developed under loading because the values of Status_XFEM of the elements at the crack tip are smaller than 1.0. Therefore the length of the elements with Status_XFEM values greater than zero is defined as the micro-crack length, which is used to indicate the crack propagation potential in this study. The micro-crack growth due to surface tension is shown in Fig. 2. It was found that for the mode-I cracking the critical crack location was located at 700-1100 mm away from tire loading.

On the other hand, the micro-crack growth due to surface shear was calculated as the crack was located at the vicinity of tire loading. It was found that the maximum shear stress caused by the load did not exceed the minimum shear stress required for crack propagation if the same shear strength is assumed as the tensile strength (1.3 MPa here). To study the influence of shear effect, the shear strength of HMA was reduced from 1.3 MPa to 0.5 MPa and the modulus of HMA was reduced from 5500 MPa to 2000 MPa, which could be the case as the temperature increased or the loading rate decreased. The effect of crack location on micro-crack length is shown in Fig. 3. The results indicate that the crack prorogation due to surface shear becomes most critical when the crack is located at the outer tire edge. This is consistent with the previous finding reported by Wang *et al*. [19]. In the repeated loading test using the asphalt pavement analyzer (APA), shear-type cracking could initiate around the loading area when the temperature was relatively higher (60℃). However, the micro-crack length for mode-II cracking is smaller than the micro-crack length for mode-I cracking even when the shear strength is reduced. Therefore, the crack propagation under surface tension is focused in the following analysis.

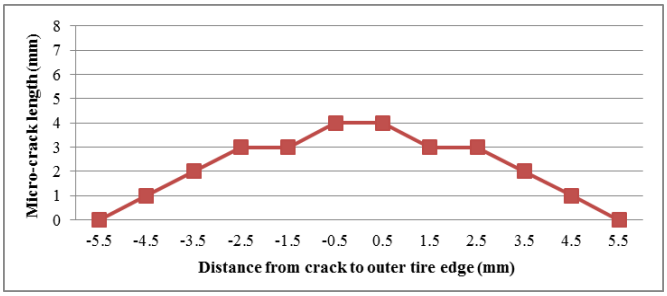

Fig. 3. Micro-crack Length Due to Shear at Different Locations (-: to the Left; +: to the Right).

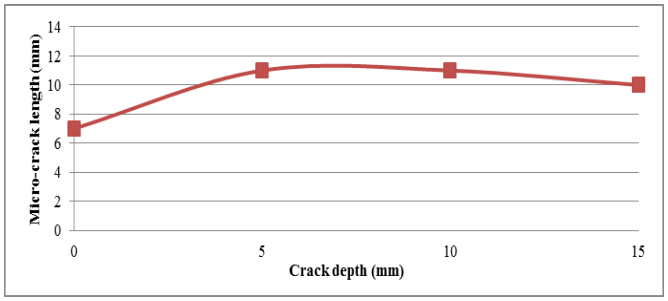

Fig. 4. Micro-crack Length as Initial Crack is Located at Different Depths.

Effect of Crack Depth

Most of the previous researches on top-down cracking focused on cracks initiated at the pavement surface and assumed that the crack propagates downward [2, 20]. However, recent field studies have indicated that the critical cracking location may not be located at the pavement surface, instead at some distances beneath the pavement surface [21, 22].

To further investigate whether the crack initiating at the near-surface grows further than the crack initiating at the pavement surface, the depth of crack was varied while the location of crack was fixed at 737 mm away from the outer tire edge. The details of the results are listed in Fig. 4. Growth of crack first increases and then decreases as the depth of crack increases from zero; there is a critical depth for crack growth at the near-surface. It can be explained from the crack propagation mechanism (Figs. 5 and 6): stress concentration occurs at the crack tip; and the crack propagates when the stress exceeds the minimum stress required for crack propagation.

For the crack at the surface, stress concentration occurs at the top of the crack and in this case the crack can only propagate in one direction. However for the crack located at some distance below the surface, stress concentration at both ends of the crack tip would allow the crack to propagate in two directions (upward and downward). The development trend of surface cracking is consistent with the findings from several field studies [20, 21]. The inspection of field cores indicated that the visible cracks could start from the top and stop at 15-22 mm below the pavement surface. The cracks did not penetrate deeper than the surface layer and some cracks were found originating at some distance from the top surface.

Effect of Crack Length and Orientation

In this part, the geometry of initial crack was altered to investigate the influence of the length and orientation of initial crack on crack propagation. Fig. 7 shows that the micro-crack length does not change much as the length of crack changes. Different crack directions may result in different stress distributions near the crack tip and possibly the mix-mode of fracture. To simulate this effect, a set of crack direction was set from 0 to 60 degrees (the angle of degree is in reference to the vertical direction) for the initial crack. Fig. 8 shows that the micro-crack length decreases as the orientation angle of the initial crack increases. This indicates that the vertical direction is the dominant direction for crack growth for mode-I fracture. This finding was supported by another field study. Taniguchi *et al*. [23] scanned the pavement specimen with a special micro-focus computer tomography (CT) scanner and vertical cracks were mostly observed throughout the upper part of the asphalt layer and the cracks were found in a scatter manner but not inter-connected.

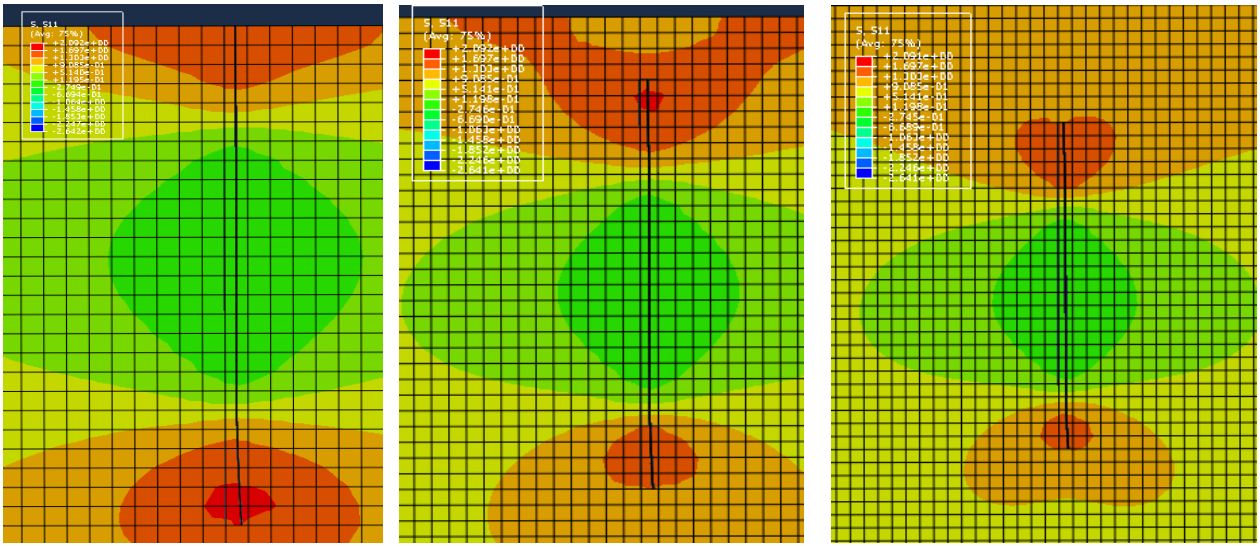

(a) (b) (c)

Fig. 5. Tensile Stress Distribution at Crack Tip as the Depth of Initial Crack is (a) 5 mm, (b) 10 mm, and (c) 15 mm.

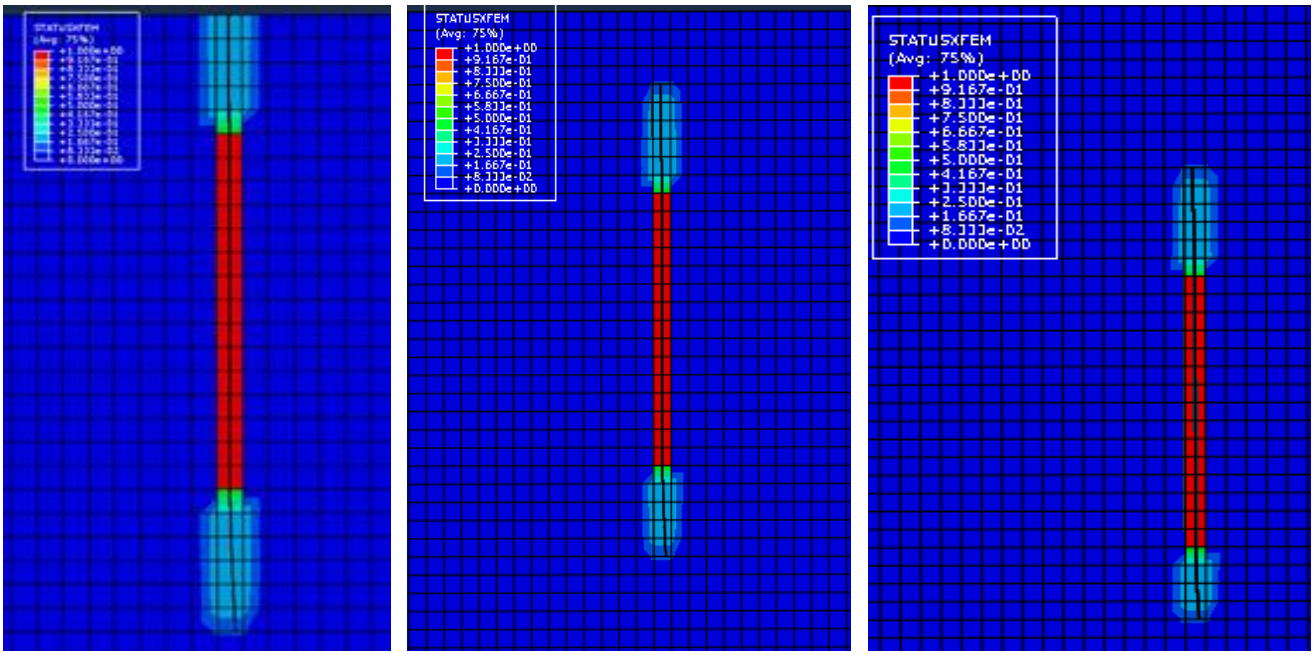

(a) (b) (c)

Fig. 6. Status_XFEM Values at Crack Tip as the Depth of Initial Crack is (a) 5 mm, (b) 10 mm, and (c) 15 mm.

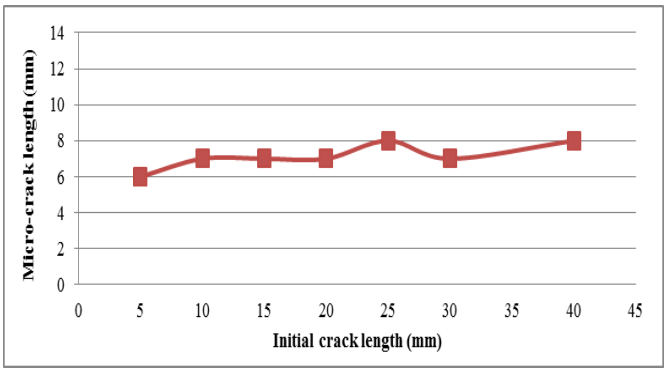

Fig. 7. Micro-crack Length at Different Initial Crack Lengths.

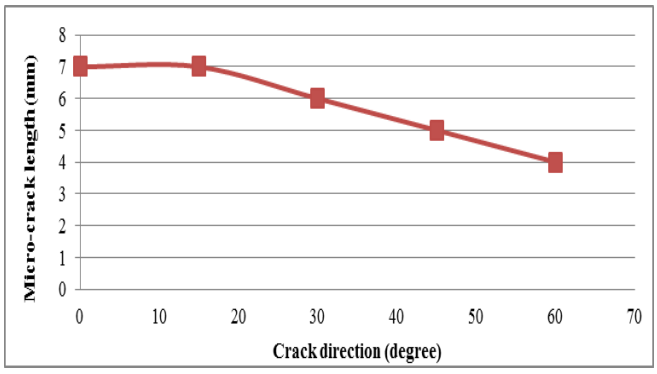

Fig. 8. Micro-crack Length at Different Crack Directions.

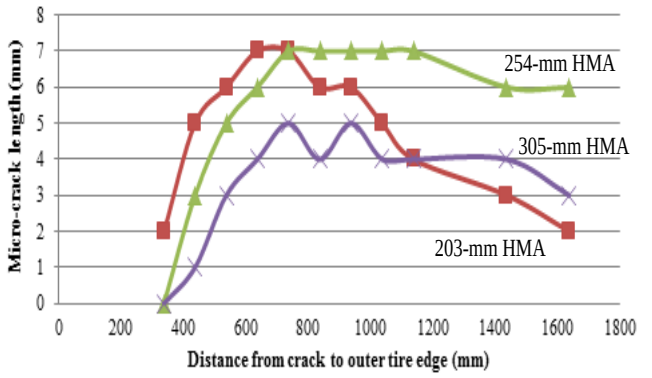

Fig. 9. Influence of HMA Layer Thickness on Micro-crack Length.

Effect of HMA Layer Thickness

The traditional pavement design demonstrates that the HMA layer thickness is a dominant factor for bottom-up cracking. To study its effect on surface initiated cracking, three HMA layer thicknesses (203, 254, and 305 mm) were analyzed and compared. Fig. 9 shows that increasing the HMA layer thickness would lead to a change in crack propagation behavior in both ways. As the HMA layer thickness increases from 203 mm to 254 mm, the micro-crack length keeps relatively constant; while as the HMA layer thickness increases from 254 mm to 305 mm, the micro-crack length decreases. This indicates that the surface initiated cracking may become most critical as the HMA layer thickness is in the intermediate range (203-254 mm).

Effect of Base and Subgrade Modulus

The pavement structure in this study is modeled as a multi-layer system. Modifying the modulus ratio between the HMA layer and the base layer changes the underlying support to the HMA layer. To study this effect, the modulus of HMA layer was kept constant and the modulus ratio of the HMA layer and the base layer was varied. The trend is shown in Fig. 10. As expected, when the base layer gets softer, the crack prorogation potential increases. However, the effect

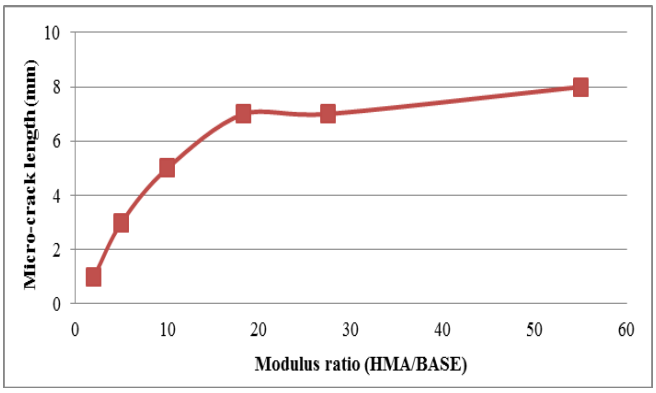

Fig. 10. Influence of Base Modulus on Micro-crack Length.

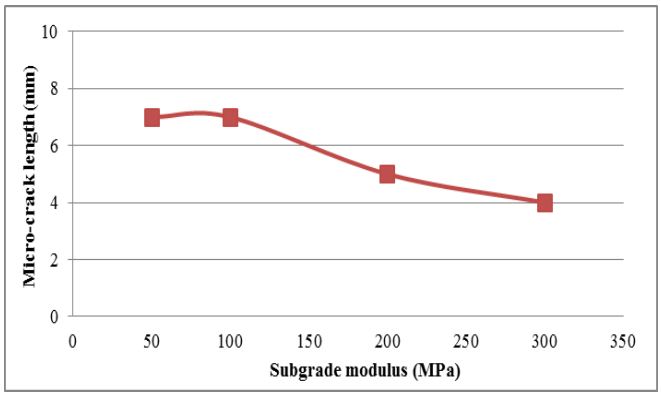

Fig. 11. Influence of Subgrade Modulus on Micro-crack Length.

of base layer becomes insignificant when the modulus ratio is greater than 20. The effect of subgrade modulus on crack propagation was evaluated using four modulus values (50, 100, 200, and 300 MPa) in the analysis. As shown in Fig. 11, stiffer subgrade results in less micro-crack growth, but the influence is not as significant as the modulus of the base layer.

Conclusions

The innovation regarding FE in this paper is the analysis of crack propagation using XFEM and cohesive zone model. With this methodology, crack propagation path does not need to be known a priori and along the element boundary that was required for traditional FEM with cohesive zone model. The crack propagation at crack tip is determined by the stress field and the crack initiation and damage evolution criteria set in the model. Although the assumptions are relatively simple regarding the tire loading and elastic material property, this study offers a parametric study on crack propagation from pavement surface or near-surface with a focus on effect of crack location and geometry.

The following conclusions were concluded from the analysis:

1. For a two-lane flexible pavement, the critical location for top-down cracking due to surface tension is 700 mm to 1100 mm away from the outer tire edge where the highest tensile stress exists. However, the critical location for top-down cracking due to surface shear is at the outer tire edge. Compared to tension effect, shear effect becomes significant as the shear strength of HMA is reduced at the high temperature. This indicates that at the intermediate temperature, surface cracking could be initiated by tension, while shear-induced cracking could happen in conjunction with rutting development at the high temperature.
2. The crack growth potential due to surface tension does not vary much as the initial crack length increases; but is affected by the depth and direction of the initial crack. The crack growth potential is most critical as the initial crack is located at some distance below pavement surface and in the purely vertical direction. As the initial crack is located at some distance below pavement surface, the crack could grow both upward and downward, which appears to be the "top-down" cracking.
3. Increasing the HMA layer thickness may not reduce surface cracking potential if the thickness of HMA layer is within the intermediate range (203-254 mm). On the other hand, higher base and subgrade modulus provide stronger support to the HMA layer and result in less crack potential when the modulus ratio of base and asphalt layer is smaller than 20 or the subgrade modulus is greater than 100 MPa.

Further study is suggested to analyze surface crack propagation using more realistic contact stress distributions and consider the heterogeneous nature of composite asphalt mixture.

References

1. Baladi, G.Y., Schorsch, M., and Svasdisant, T. (2003). *Determining the Causes of Top-Down Cracks in Bituminous Pavements*, Pavement Research Center of Excellence, Department of Civil and Environmental, Michigan State University, East Lansing, Michigan, USA.
2. Myers, L.A., Roque, R., and Birgisson, B. (2001). Propagation Mechanisms for Surface-Initiated Longitudinal Wheelpath Cracks, *Transportation Research Record*, No. 1778, pp. 113-12.
3. Al-Qadi, I., Wang, H., Yoo, P., and Dessouky, S.H. (2008). Dynamic Analysis and In Situ Validation of Perpetual Pavement Response to Vehicular Loading, *Transportation Research Record*, No. 2087, pp. 29-39.
4. Wang, H. and Al-Qadi, I.L. (2009). Combined Effect of Moving Wheel Loading and Three-Dimensional Contact Stresses on Perpetual Pavement Responses, *Transportation Research Record*, No. 2095, pp. 53-61.
5. Wang, H. and Al-Qadi, I.L. (2010). Near-Surface Pavement Failure Under Multiaxial Stress State in Thick Asphalt Pavement, *Transportation Research Record*, No. 2154, pp. 91-99.
6. Jeng, Y. and Perng, J. (1991). Analysis of Crack Propagation in Asphalt Concrete Using Cohesive Crack Model, *Transportation Research Record*, No. 1317, pp. 90-99.
7. Song, S., Paulino, G.H., and Buttlar, W.G. (2006). Simulation of Crack Propagation in Asphalt Concrete Using an Intrinsic Cohesive Zone Model, *Journal of Engineering Mechanics*, 132(11), pp. 1215-1223.
8. Belytschko, T. and Black, T. (1999). Elastic Crack Growth in Finite Elements with Minimal Remeshing, *International Journal for Numerical Methods in Engineering*, 45(5), pp. 601-620.

9. Ozer, H., Al-Qadi, I., and Duarte, C. (2011). A Three-Dimensional Generalized Finite Element Analysis for the Near-Surface Cracking Problem in Flexible Pavements, *International Journal of Pavement Engineering*, 12(4), pp. 407-419.
10. Garzon, J., Duarte, C., and Buttlar, W. (2010). Analysis of Reflective Cracks in Airfield Pavements using a 3-D Generalized Finite Element Method, *Road Materials and Pavement Design*, 11(2), pp. 459-477.
11. Duarte, C., Babuska, I., and Oden, J. (2000). Generalized Finite Element Methods for Three Dimensional Structural Mechanics Problems, *Computers and Structures*, 77(2), pp. 215-232.
12. Babuska, I. and Melenk, J. (1997). The Partition of Unity Method, *International Journal for Numerical Methods in Engineering*, 40(4), pp. 727-758.
13. Osher, S.J. and Fedkiw, R.P. (2002). *Level Set Methods and Dynamic Implicit Surfaces*, Springer-Verlag, Berlin, Germany.
14. Song, J., Areias, P., and Belytschko, T. (2006). A Method for Dynamic Crack and Shear Band Propagation with Phantom Nodes, *International Journal for Numerical Methods in Engineering*, 67(6), pp. 868-893.
15. ABAQUS (2005). *ABAQUS/Standard User's Manual*,Version 6.10, Habbit, Karlsson & Sorenson, Inc., Pawtucket, Rhode Island, USA.
16. Im, S., Ban, H., and Kim, Y.-R. (2013). Characterization of Mode-I and Mode-II Fracture Properties of Asphalt Mixture Using Semicircular Specimen Geometry, *Proceeding of the 92nd Annual Meeting of Transportation Research Board*, Washington, DC, USA.
17. Bensalem, A., Broen, A.J., Nunn, M.E., Merrill, D.B., and Lloyd, W.G. (2002). Finite Element Modeling of Fully Flexible Pavements: Surface Cracking and Wheel Interaction, *Proceedings of the 2nd International Symposium on 3D Finite Element for Pavement Analysis, Design, and Research*, pp. 103-121, Charleston, West Virginia, USA.
18. Mohammad, F.A., Collop, A.C., and Brown, S.F. (2005). Effects of Surface Cracking on Responses in Flexible Pavements, *Proceedings of the Institution of Civil Engineers Transport*, Vol. 158, pp. 127-134.
19. Wang, L.B., Myers, L.A., Mohammad, L.N., and Fu, Y.R. (2003). Micromechanics Study on Top-Down Cracking, *Transportation Research Record*, No. 1853, pp. 121-133.
20. Collop, A. and Cebon, D. (1995). A Theoretical Analysis of Fatigue Cracking in Flexible Pavements, *Proceedings of the Institution of Mechanical Engineers Part C - Journal of Mechanical Engineering Science*, 209(5), pp. 345-361.
21. Pellinen, T., Rowe, G., and Biswas, K. (2004). Evaluation of Surface (Top Down) Longitudinal Wheel Path Cracking, *Final Report: FHWA/IN/JTRP-2004/6*, Joint Transportation Research Program, Department of Transportation and Purdue University, West Lafayette, Indiana, USA.
22. Uhlmeyer, J.S., Willoughby, K., Pierce, L.M., and Mahoney, J.P. (2000). Top-Down Cracking in Washington State Asphalt Concrete Wearing Courses, *Transportation Research Record*, No. 1730, pp. 110-116.
23. Taniguchi, S., Nishizaki, I., and Moriyoshi, A. (2008). A Study of Longitudinal Cracking in Asphalt Pavement Using CT Scanner, *Road Material and Pavement Design*, 9(3), pp. 549-558.